Mathematical and Computer Modelling 52 (2010) 501–514

Contents lists available at ScienceDirect

Mathematical and Computer Modelling

journal homepage: www.elsevier.com/locate/mcm

Peristaltic transport of a visco-elastic fluid in a tube of non-uniform cross section

S.K. Pandey*, M.K. Chaube

Department of Applied Mathematics, Institute of Technology, Banaras Hindu University, 221005 Varanasi, Uttar Pradesh, India

ARTICLE INFO

Article history:
Received 2 June 2009
Received in revised form 22 March 2010
Accepted 22 March 2010

Keywords:
Peristalsis
Axi-symmetric flow
Maxwell fluid
Non-uniform tube
Spermatic flow
Vas deferens

ABSTRACT

In this paper, the axi-symmetric peristaltic transport of a viscous incompressible visco-elastic fluid has been investigated through a circular tube whose cross section changes along the length. The wall motion is governed by a wave of contraction propagating along the wall of the tube which contracts in the radial direction and then relaxes up to the boundary of the fully distended tube. The nonlinear convective acceleration terms have been duly considered for non-creeping flow. A perturbation technique has been employed to analyze the problem. This paper is concerned with two particular cases: (i) Reynolds number is small and (ii) the wave number is small. The extensive analysis is based upon second order approximation. The effects of the non-Newtonian parameter relaxation time on the flow rate and the mean axial velocity have been analyzed. The derived analytical expressions have been computed in order to carry out a comprehensive investigation of an important physiological problem, i.e. spermatic flow through the vas deferens, in which peristalsis has a role to play. It is concluded that flow rate decreases with relaxation time and increases with Reynolds number while pressure increases with relaxation time and decreases with Reynolds number at a given tapering.

1. Introduction

The natural phenomenon by means of which fluids are transported within human body from one place to another is termed as peristaltic motion in which the required pressure gradient for flow is induced by progressive waves of area contraction or expansion along the length of the distensible tube containing fluid. Peristaltic motion occurs in blood flow through blood vessels, urine flow through ureter, chyme flow through gastrointestinal tract, bile flow through bile duct and spermatic fluid flow through vas deferens, etc. Some worms also use peristaltic motion as a means of locomotion. Roller and finger pumps using viscous fluids also operate on this principle. Since the first investigation made by Latham [1], several researchers have made attempts to investigate peristaltic motion of different types of fluids through different geometries.

Most of the theoretical investigations have been carried out by assuming physiological fluids as Newtonian or non-Newtonian fluid by neglecting inertia terms. It is a known fact that most of the physiological fluids behave like a non-Newtonian fluid (e.g., blood, chyme and spermatic fluid). Gupta and Seshadri [2] analyzed the peristaltic flow through non-uniform channels and tubes with particular reference to the flow of spermatic fluid in vas deferens, neglecting the inertia terms. Srivastava and Srivastava [3,4] carried out extensions of the analyses by considering the spermatic fluid as power law fluid in uniform and non-uniform two-dimensional tubes and channels respectively for zero Reynolds number which neglects inertia terms. Misra and Pandey [5] further extended the analysis by considering spermatic fluid as Newtonian fluid but duly keeping inertia terms into account. Eytan et al. [6] studied peristaltic transport of embryo within

* Corresponding author. Tel.: +91 9450533132.
E-mail address: skpandey.apm@itbhu.ac.in (S.K. Pandey).

0895-7177/$ – see front matter © 2010 Elsevier Ltd. All rights reserved.
doi:10.1016/j.mcm.2010.03.047

Nomenclature

z	axial coordinate
r	radial coordinate
a	radius of the tube
a_0	radius of the tube at inlet
ρ	density
υ	kinematic viscosity
H	wall-displacement
c	wave velocity
b	amplitude of the wave
t	time parameter
t_m	relaxation time
ε	amplitude ratio
w	axial velocity
υ	radial velocity
p	pressure
λ	wavelength
ψ	stream function

the uterin cavity in a tapered channel; Mekheimer [7,8] investigated respectively peristaltic flow of couple stress fluid and couple stress fluid under the effect of a magnetic field for blood in uniform/non-uniform channels; Mekheimer [9] studied peristalsis of Newtonian fluids in an annulus and Mekheimer and Elmaboud [10] extended it for particle-fluid suspension; Sobh [11] introduced slip effects on couple stress fluid; and Hariharan et al. [12] examined effects of different wave forms on peristaltic transport of non-Newtonian fluids. They all applied long wavelength approximations for analysis whereas Ali et al. [13] studied peristaltic flow of a Maxwell fluid in a channel with compliant walls by employing perturbation technique.

We opine that the flow within vas deferens is axi-symmetric and not creeping one, nor is the Reynolds number zero. So, there is no point to consider the flow inertia free. Further, Srivastava and Srivastava [3] refer to the observation of Maharenholtz et al. [14], who state that the shape of the wave on the wall has almost negligible affect on the zero Reynolds number theory. Here, the wave equation will have an impact on the flow since the Reynolds number is not zero. Moreover, the wall never expands beyond its fully stretched distended geometry; so a modification that confines the radial motion to contraction and relaxation, is required. Another modification to spermatic flow seems to be related with the physical property of the fluid. A visco-elastic model will represent the flow in a better way than the Newtonian model or even the power-law model which is more suitable for the flow of chyme in the small intestine.

In this paper, we analyze the peristaltic flow of a non-Newtonian Maxwell fluid through a flexible tube of changing cross section, where the nonlinear convective acceleration terms are duly considered as they are comparable with the viscous terms.

2. Mathematical model of the problem

We consider the axi-symmetric flow of an incompressible visco-elastic fluid through a circular cylindrical diverging tube. The governing equations for a visco-elastic fluid described by Maxwell model may be given by

$$\left(1+t_m\frac{\partial}{\partial t}\right)\left(\frac{\partial}{\partial t}+u\frac{\partial}{\partial r}+w\frac{\partial}{\partial z}\right)u=-\frac{1}{\rho}\left(1+t_m\frac{\partial}{\partial t}\right)\frac{\partial p}{\partial r}+\nu\left(\frac{\partial^2}{\partial r^2}+\frac{\partial^2}{\partial z^2}+\frac{1}{r}\frac{\partial}{\partial r}-\frac{1}{r^2}\right)u \tag{1}$$

$$\left(1+t_m\frac{\partial}{\partial t}\right)\left(\frac{\partial}{\partial t}+u\frac{\partial}{\partial r}+w\frac{\partial}{\partial z}\right)w=-\frac{1}{\rho}\left(1+t_m\frac{\partial}{\partial t}\right)\frac{\partial p}{\partial z}+\nu\left(\frac{\partial^2}{\partial r^2}+\frac{\partial^2}{\partial z^2}+\frac{1}{r}\frac{\partial}{\partial r}\right)w \tag{2}$$

$$\frac{\partial u}{\partial r}+\frac{\partial w}{\partial z}+\frac{u}{r}=0, \tag{3}$$

where t_m is the relaxation time, t is the time parameter, u and w are the radial and axial velocities respectively, r and z are the radial and the axial coordinates, ρ and υ are the density and the kinematic viscosity of the fluid, p is the pressure.

The following progressive contraction waves of small amplitude are assumed to propagate along on the wall of the tube:

$$H(z,t)=a(z)-b\cos^2\frac{\pi}{\lambda}(z-ct), \tag{4}$$

where H is the wall-displacement, $a(z)$ the radius of the tube, b the amplitude of the wave, λ the wavelength and c the wave velocity. The Eq. (4) permits contraction and relaxation but does let the wall move beyond its natural boundary. This matches wall motion of physiological ducts.

The stream function ψ satisfying the continuity equation (3) is given by

$$u = \frac{1}{r}\frac{\partial \psi}{\partial z}, \qquad w = -\frac{1}{r}\frac{\partial \psi}{\partial r}. \tag{5}$$

Eliminating pressure terms from Eqs. (1) and (2) and then using Eq. (5), we find that the governing equations reduce to

$$\left(1 + t_m \frac{\partial}{\partial t}\right)\left[\frac{\partial}{\partial t}\mathrm{D}^2\psi - r\frac{\partial\left\{\psi, \left(1/r^2\right)\mathrm{D}^2\psi\right\}}{\partial\left(r, z\right)}\right] = \upsilon \mathrm{D}^4\psi \tag{6}$$

where $\mathrm{D}^2 \equiv \frac{\partial^2}{\partial r^2} - \frac{1}{r}\frac{\partial}{\partial r} + \frac{\partial^2}{\partial z^2}$.

We non-dimensionalize various quantities as follows:

$$H' = \frac{H}{a_0}, \qquad a' = \frac{a}{a_0}, \qquad r' = \frac{r}{a_0}, \qquad z' = \frac{z}{a_0}, \qquad u' = \frac{u}{c}, \qquad w' = \frac{w}{c},$$
$$t' = \frac{ct}{a_0}, \qquad t'_m = \frac{ct_m}{a_0}, \qquad \psi' = \frac{\psi}{ca_0^2}, \qquad p' = \frac{p}{\rho c^2}, \qquad \alpha = \frac{2\pi\, a_0}{\lambda}, \qquad R = \frac{ca_0}{\upsilon}, \qquad \varepsilon = \frac{b}{a_0}, \tag{7}$$

where a_0 is the radius of the tube at inlet. Dropping the primes we get

$$\left\{\frac{1}{R}\mathrm{D}^2 - \left(1 + t_m\frac{\partial}{\partial t}\right)\frac{\partial}{\partial t}\right\}\mathrm{D}^2\psi = \left(1 + t_m\frac{\partial}{\partial t}\right)\left(\frac{1}{r}\frac{\partial\psi}{\partial z}\frac{\partial}{\partial r}\mathrm{D}^2\psi - \frac{1}{r}\frac{\partial\psi}{\partial r}\frac{\partial}{\partial z}\mathrm{D}^2\psi - \frac{2}{r^2}\frac{\partial\psi}{\partial z}\mathrm{D}^2\psi\right). \tag{8}$$

The regularity conditions at the centre of the pipe, $r = 0$, are

$$u = 0, \quad \text{and } w \text{ is finite.} \tag{9}$$

On the wall, $r = a - \varepsilon\cos^2\frac{\alpha}{2}\left(z - t\right)$, the tangential motion of the wall is assumed to be negligible. So the impermeability condition gives

$$u = \frac{1}{r}\frac{\partial\psi}{\partial z} = -\frac{\alpha}{2}\varepsilon\sin\alpha\left(z - t\right), \qquad w = -\frac{1}{r}\frac{\partial\psi}{\partial r} = 0. \tag{10}$$

For a slightly tapered tube, representing the stream function ψ as a power series in the amplitude ratio, we have

$$\psi = \psi_0 + \varepsilon\psi_1 + \varepsilon^2\psi_2 + \cdots, \tag{11}$$

in which ψ_0 represents stream function for the original flow (i.e. the flow before the peristalsis occurs) which, at any cross section is assumed to be local Hagen–Poiseuille flow, given by

$$w_0 = k_0\left(a^2 - r^2\right) \tag{12}$$

where $k_0 = -\frac{R}{4}\left(\frac{\mathrm{d}p}{\mathrm{d}z}\right)_0 = \frac{1}{h^4}\frac{2Q_0}{\pi\, a_0^2 c}$, Q_0 being the instantaneous volume flow rate.

When the traveling wave is imposed on the wall, the pressure gradient and the flow rate may be assumed to be functions of ε in the form of a series

$$-\frac{R}{4}\frac{\mathrm{d}p}{\mathrm{d}z} \equiv k = k_0 + \varepsilon\, k_1 + \varepsilon^2 k_2 + \cdots, \tag{13}$$

$$Q = Q_0 + \varepsilon\, Q_1 + \varepsilon^2 Q_2 + \cdots, \tag{14}$$

where $k_1, k_2, \ldots, Q_1, Q_2, \ldots, etc.$ correspond to peristalsis.

Substituting Eqs. (11) and (12) in Eq. (8) and equating the coefficients of ε and ε^2, we obtain

$$\frac{1}{R}\mathrm{D}^4\psi_1 = \left(1 + t_m\frac{\partial}{\partial t}\right)\left[\frac{\partial}{\partial t} + k_0\left(a^2 - r^2\right)\frac{\partial}{\partial z}\right]\mathrm{D}^2\psi_1, \tag{15}$$

$$\left[\frac{1}{R}\mathrm{D}^2 - \left(1 + t_m\frac{\partial}{\partial t}\right)\frac{\partial}{\partial t} - k_0\left(a^2 - r^2\right)\frac{\partial}{\partial z}\right]\mathrm{D}^2\psi_2 = \left(1 + t_m\frac{\partial}{\partial t}\right)\left[u_1\left(\frac{\partial}{\partial r} - \frac{2}{r}\right) + w_1\frac{\partial}{\partial z}\right]\mathrm{D}^2\psi_1. \tag{16}$$

Setting

$$\Phi = \frac{\psi}{r}, \quad \text{So that } u = \frac{\partial\Phi}{\partial z}, \qquad w = -\left(\frac{\partial\Phi}{\partial r} + \frac{\Phi}{r}\right), \tag{17}$$
$$\Phi = \Phi_0 + \varepsilon\,\Phi_1 + \varepsilon^2\Phi_2 + \cdots.$$

The boundary conditions (10) become at $r = a$.

$$\begin{aligned} \varepsilon:\quad & \Phi_{1z} = -\frac{\alpha}{2}\sin\alpha\,(z-t) \\ & \Phi_{1r} + \frac{\Phi_1}{r} = 2k_0 a\cos^2\frac{\alpha}{2}\,(z-t)\,. \end{aligned} \tag{18}$$

$$\begin{aligned} \varepsilon^2:\quad & \Phi_{2z} - \Phi_{1zr}\cos^2\frac{\alpha}{2}\,(z-t) = 0, \\ & \Phi_{2r} + \frac{\Phi_2}{r} - \left(\Phi_{1r} + \frac{\Phi_1}{r}\right)_r \cos^2\frac{\alpha}{2}\,(z-t) = -k_0\cos^4\frac{\alpha}{2}\,(z-t)\,, \end{aligned} \tag{19}$$

while the regularity conditions (9) become

$$\Phi_1 = 0, \quad \Phi_{1r} \text{ is finite,} \tag{20}$$

$$\Phi_2 = 0, \quad \Phi_{2r} \text{ is finite.} \tag{21}$$

We substitute

$$\left.\begin{aligned} \Phi_1 &= \phi_1(r)\cos\alpha\,(z-t) + \phi_2(r)\sin\alpha\,(z-t)\,, \\ \Phi_2 &= \phi_3(r) + \phi_4(r)\cos 2\alpha\,(z-t) + \phi_5(r)\sin 2\alpha\,(z-t)\,. \end{aligned}\right\} \tag{22}$$

Similarly,

$$\left.\begin{aligned} Q_1 &= Q_{11}(r)\cos\alpha\,(z-t) + Q_{12}(r)\sin\alpha\,(z-t)\,, \\ Q_2 &= Q_{20}(r) + Q_{21}(r)\cos 2\alpha\,(z-t) + Q_{22}(r)\sin 2\alpha\,(z-t)\,. \end{aligned}\right\} \tag{23}$$

The Eq. (15) reduces to

$$L_\alpha^2(\phi_1) - R\alpha\left\{k_0\left(a^2 - r^2\right) - 1\right\}L_\alpha(\phi_2) - R\alpha^2 t_m\left\{k_0\left(a^2 - r^2\right) - 1\right\}L_\alpha(\phi_1) = 0, \tag{24}$$

$$L_\alpha^2(\phi_2) + R\alpha\left\{k_0\left(a^2 - r^2\right) - 1\right\}L_\alpha(\phi_1) - R\alpha^2 t_m\left\{k_0\left(a^2 - r^2\right) - 1\right\}L_\alpha(\phi_2) = 0 \tag{25}$$

where

$$L_\alpha = \frac{\mathrm{d}^2}{\mathrm{d}r^2} + \frac{1}{r}\frac{\mathrm{d}}{\mathrm{d}r} - \left(\frac{1}{r^2} + \alpha^2\right) = L_0 - \alpha^2.$$

The time averaged mean flow over an interval of an oscillating period gives the mean flow. We have

$$\Phi = \Phi_0 + \varepsilon^2\overline{\Phi}_2 = \phi_0 + \varepsilon^2\phi_3, \tag{26}$$

$$w = w_0 + \varepsilon^2\overline{\omega_2,} \tag{27}$$

$$k = k_0 + \varepsilon^2\overline{k_2} \tag{28}$$

and

$$\overline{Q} = Q_0 + \varepsilon^2 Q_{20}. \tag{29}$$

Substituting (22) in to (16) and using (17), the differential equation for ϕ_3 is found to be

$$L_0^2(\phi_3) = \frac{\alpha R}{2}\frac{\mathrm{d}}{\mathrm{d}r}\left[\phi_2 L_\alpha(\phi_1) - \phi_1 L_\alpha(\phi_2)\right]. \tag{30}$$

As $R \to 0$ (Stokes Approximation) it is obvious that

$$L_\alpha^2(\phi_1) = 0, \qquad \phi_2 = 0 \quad \text{and} \quad L_0^2(\phi_3) = 0. \tag{31}$$

Hence the solution may be expected to be of the form

$$\left.\begin{aligned} \phi_1 &= \phi_{10} + R^2\phi_{12} + \cdots, \\ \phi_2 &= R\phi_{21} + O\left(R^3\right) + \cdots, \\ \phi_3 &= \phi_{30} + R^2\phi_{32} + \cdots \end{aligned}\right\} \tag{32}$$

and

$$k_2 = \overline{k}_{20} + R^2\overline{k}_{22} + \cdots. \tag{33}$$

3. Creeping flow

This is a situation in which the Reynolds number is considered so small that the inertia terms in the governing equations are negligible. Here we have to find only $\phi_{10}(r)$ and $\phi_{30}(r)$. From Eqs. (24) and (18), we have

$$L_\alpha^2\left[\phi_{10}\left(r\right)\right]=0, \tag{34}$$

$$\phi_{10}\left(a\right)=\frac{1}{2},\qquad \phi_{10}'\left(a\right)=\frac{k_0 a}{2}-\frac{1}{2a}. \tag{35}$$

The solution of (34) satisfying the regularity condition (20) is given by

$$\phi_{10}\left(r\right)=A_0 r I_0\left(\alpha\, r\right)+B_0 I_1\left(\alpha\, r\right), \tag{36}$$

where A_0 and B_0 evaluated from (35) are given by

$$A_0=\frac{\alpha\, I_0-k_0 a I_1}{2\Delta},\qquad B_0=-\frac{\left\{\left(2-k_0 a^2\right)I_0+a\alpha\, I_1\right\}}{2\Delta} \tag{37}$$

where $\Delta=a\alpha\left(I_0^2-I2_1\right)-2I_0 I_1$, and $I_0, I_1, \ldots, etc.$ stand for $I_0\left[a\alpha\right], I_1\left[a\alpha\right], \ldots$.

Eq. (30) and the associated boundary condition at $r=a$, reduce, respectively, to

$$L_0^2\left[\phi_{30}\left(r\right)\right]=0 \tag{38}$$

and

$$\phi_{30}'\left(a\right)+\frac{\phi_{30}(a)}{a}=H\left(a\right) \tag{39}$$

where $H\left(a\right)$ is defined as

$$H\left(a\right)=\frac{1}{4}\left\{\phi_{10}''\left(a\right)-\frac{1}{a^2}-k_0\right\} \tag{40}$$

$$\phi_{10}''\left(a\right)=\frac{\alpha I_1\left(\alpha\, I_0-k_0 a I_1\right)}{\Delta}+\frac{1}{2}\left(\frac{2}{a^2}-k_0+\alpha^2\right), \tag{41}$$

$\phi_{30}\left(r\right)$ further satisfies (21) at $r=0$. Thus

$$\phi_{30}\left(r\right)=C_0 r^3+E_0 r. \tag{42}$$

From (17) and (39), we have

$$\varpi_2\left(r\right)=2E_0\left\{\left(\frac{r}{a}\right)^2-1\right\}-\frac{r^2}{a^2}H\left(a\right), \tag{43}$$

where the constant E_0 is arbitrary, which may be related to the mean value of k_2; i.e.,

$$\bar{k}_{20}=\frac{2E_0-H\left(a\right)}{a^2}. \tag{44}$$

Therefore,

$$\varpi_2\left(r\right)=a^2\bar{k}_{20}\left\{\left(\frac{r}{a}\right)^2-1\right\}-H\left(a\right) \tag{45}$$

and so

$$\varpi\left(r\right)=\left(k_0+\varepsilon^2\overline{k_{20}}\right)a^2\left\{1-\left(\frac{r}{a}\right)^2\right\}-\varepsilon^2 H\left(a\right). \tag{46}$$

4. Non-creeping flow

It is clear from (32) that the main correction due to increasing Reynolds number is $\phi_{32}\left(r\right)$.

But from (30) it is evident that before getting $\phi_{32}\left(r\right)$, the functions $\phi_{12}\left(r\right)$ and $\phi_{21}\left(r\right)$ should be found. For these functions, the equations and the boundary conditions at $r=a$ are, to the order R, from (25) and (18), we obtain

$$L_\alpha^2\left[\phi_{21}\left(r\right)\right]=-\alpha\left[k_0\left(a^2-r^2\right)-1\right]L_\alpha\left(\phi_{10}\left(r\right)\right), \tag{47}$$

$$\phi_{21}\left(a\right)=\phi_{21}'\left(a\right)=0.$$

To the order R^2, from (24) and (18), we have

$$L_\alpha^2\left[\phi_{12}\left(r\right)\right]=\alpha\left[k_0\left(a^2-r^2\right)-1\right]L_\alpha\left(\phi_{21}\left(r\right)\right)+\frac{1}{R}\alpha^2 t_m\left[k_0\left(a^2-r^2\right)-1\right]L_\alpha\left(\phi_{10}\right) \tag{48}$$

$$\phi_{12}\left(a\right)=\phi_{12}'\left(a\right)=0.$$

From (30) and (18), we get

$$L_0^2\left[\phi_{32}\left(r\right)\right]=\frac{\alpha}{2}\frac{\mathrm{d}}{\mathrm{d}r}\left[\phi_{21}L_\alpha\left(\phi_{10}\right)-\phi_{10}L_\alpha\left(\phi_{21}\right)\right]. \tag{49}$$

$$\phi_{32}'\left(a\right)+\frac{\phi_{32}\left(a\right)}{a}=\frac{1}{4}\phi_{12}''\left(a\right).$$

In addition, $\phi_{21}\left(r\right)$ and $\phi_{12}\left(r\right)$ should satisfy (20) and (21) at the centre of the pipe. The foregoing differential equations posses non-homogeneous solutions with their homogeneous parts found in the previous section ($R=0$).

From Eq. (47), we get

$$\phi_{21}\left(r\right)=A_1 rI_0\left(\alpha r\right)+B_1 I_1\left(\alpha r\right)+\phi_{21p}\left(r\right), \tag{50}$$

where the particular solution is

$$\phi_{21p}\left(r\right)=\frac{A_0}{24}r^2 I_3\left(\alpha r\right)\left[6\left(1-k_0a^2\right)+k_0r^2\right],$$

and the constants A_1 and B_1 are given by

$$A_1=\frac{A_0}{24\Delta}a^2\left[\alpha\left(6-5k_0a^2\right)\left(I_1I_2-I_0I_3\right)+2k_0aI_1I_3\right],$$

$$B_1=\frac{A_0}{24\Delta}a^2\left[a\alpha\left(6-5k_0a^2\right)\left(I_1I_3-I_0I_2\right)+12\left(1-k_0a^2\right)I_0I_3\right].$$

The solution of (48) may be written as

$$\begin{aligned}\phi_{12}\left(r\right)=&\ A_2 rI_0\left(\alpha r\right)+B_2 I_1\left(\alpha r\right)-\frac{A_1}{24}r^2 I_3\left(\alpha r\right)\left\{6\left(1-k_0a^2\right)+k_0r^2\right\}\\ &-\frac{A_0}{12}\left[\left(1-k_0a^2\right)r^3 I_4\left(\alpha r\right)\left(\frac{1-k_0a^2}{2}+\frac{k_0r^2}{5}\right)+\frac{k_0^2}{5\alpha}a^2r^6 I_5\left(\alpha r\right)+\frac{k_0^2}{42}r^7 I_6\left(\alpha r\right)\right]\\ &-\frac{A_0}{24}\frac{t_m\alpha}{R}r^2 I_3\left(\alpha r\right)\left[6\left(1-k_0a^2\right)-k_0r^2\right]\end{aligned}$$

where

$$\begin{aligned}A_2=&-\frac{A_1^2}{A_0}-\frac{A_0a^3}{120\alpha\Delta}\Bigg[\left(1-k_0a^2\right)\alpha^2\left(5-3k_0a^2\right)\left(I_1I_3-I_0I_4\right)\\ &+a\alpha\left\{2k_0^2a^4+4k_0\left(1-k_0a^2\right)\right\}I_1I_4-2k_0^2a^5\alpha I_0I_5+\left(4+\frac{5}{21}\alpha^2\right)k_0^2a^4I_1I_5+\frac{5}{21}\alpha\,k_0^2a^3\left(2I_1I_6-a\alpha I_0I_6\right)\Bigg]\\ &-\frac{A_0}{24\Delta}\frac{t_m\alpha}{R}a^2\left[\alpha\left(6-5k_0a^2\right)\left(I_1I_2-I_0I_3\right)+2k_0aI_1I_3\right]\\ B_2=&-\frac{A_1B_1}{A_0}-\frac{A_0a^3}{120\alpha\Delta}\Bigg[a\alpha^2\left(1-k_0a^2\right)\left(5-3k_0a^2\right)\left(I_1I_4-I_0I_3\right)\\ &+\left\{10\left(1-k_0a^2\right)^2-2k_0^2a^6\right\}\alpha I_0I_4+\alpha\,k_0^2a^5\left\{2aI_1I_5+\frac{5}{21}\alpha\left(I_1I_6-I_0I_5\right)\right\}\Bigg]\\ &+\frac{A_0}{24}\frac{t_m\alpha}{R\Delta}a^2\left[a\alpha\left(6-5k_0a^2\right)\left(I_0I_2-I_1I_3\right)-2I_0I_3\left(6-5k_0a^2\right)\right].\end{aligned}$$

Hence, we have

$$\begin{aligned}\phi_{12}''\left(a\right)=&\ A_2\alpha\left(I_1+a\alpha\,I_0\right)+B_2\left\{\left(\alpha^2+\frac{2}{a^2}\right)I_1-\frac{\alpha}{a}I_0\right\}\\ &-\frac{A_1}{2}\left[\left(1-k_0a^2\right)I_3-\frac{1}{4}\left(2-3k_0a^2\right)a\alpha\,I_2+\frac{1}{12}\left(6-5k_0a^2\right)a^2\alpha^2I_1\right]\\ &-\frac{A_0}{120}\Bigg[\left(1-k_0a^2\right)\left(5-3k_0a^2\right)a^3\alpha^2I_2+\left(16k_0a^2-11k_0^2a^4+2k_0^2a^6-5\right)a^2\alpha\,I_3\\ &+\left\{10\left(1-k_0a^2\right)^2a\alpha+6k_0^2a^7+\frac{5}{21}k_0^2\alpha^2a^7\right\}I_4+\frac{5}{7}\alpha\,k_0^2a^6I_5\Bigg]\\ &-\frac{A_0}{24}\frac{t_m\alpha}{R}\left[a^2\alpha^2I_1-3a\alpha\,I_2\left(2-3k_0a^2\right)+3I_3\left(4-7k_0a^2+3k_0a^3\right)\right].\end{aligned} \tag{51}$$

This is needed in the solution of (49).

We write Eq. (49) as

$$L_0^2\left[\phi_{32}\left(r\right)\right]=\frac{\mathrm{d}}{\mathrm{d}r}f\left(r\right) \tag{52}$$

where

$$f\left(r\right)=\alpha^2\left[\left(A_0B_1-A_1B_0\right)I_1^2\left(\alpha\, r\right)+\frac{1}{4}A_0^2r^2I_1\left(\alpha\, r\right)I_3\left(\alpha\, r\right)\left(1-k_0a^2+\frac{k_0}{6}r^2\right)\right.$$
$$\left.-\frac{A_0}{2}I_2\left(\alpha\, r\right)r\left(1-k_0a^2+\frac{k_0}{3}r^2\right)\left(A_0rI_0\left(\alpha\, r\right)+B_0I_1\left(\alpha\, r\right)\right)\right].$$

Putting $\Theta\equiv r\frac{\mathrm{d}}{\mathrm{d}r}$, the solution of (52) is given by

$$\phi_{32}\left(r\right)=C_2r^3+E_2r+\frac{1}{16}\left[\frac{1}{\Theta-3}-\frac{1}{\Theta+1}-\frac{4}{\left(\Theta-1\right)^2}\right]\left\{r^4\frac{\mathrm{d}}{\mathrm{d}r}f\left(r\right)\right\}$$
$$=C_2r^3+E_2r+\frac{1}{4}\left[\frac{1}{r}\int_0^r t^3f\left(t\right)\mathrm{d}t-r\int_0^r tf\left(t\right)\mathrm{d}t+2r\int_0^r t^{-1}\int_0^t sf\left(s\right)\mathrm{d}s\mathrm{d}t\right]. \tag{53}$$

Following the same argument as that given in the derivation of (44), we get

$$\varpi_2\left(r\right)=-H\left(a\right)\left(\frac{r}{a}\right)^2-2\left(E_0+R^2E_2\right)\left\{1-\left(\frac{r}{a}\right)^2\right\}-R^2\left[\left\{\frac{1}{4}\phi_{12}''\left(a\right)-\beta\left(a\right)\right\}\left(\frac{r}{a}\right)^2+\beta\left(r\right)\right]$$

where

$$\beta\left(r\right)=\int_0^r t^{-1}\int_0^t sf\left(s\right)\mathrm{d}s\mathrm{d}t.$$

$\overline{k_2}$, given in (33), may be presented in the modified form as

$$\bar{k}_2=-\left[-\frac{H\left(a\right)}{a^2}+\frac{2}{a^2}\left(E_0+R^2E_2\right)-\frac{R^2}{a^2}\left\{\frac{1}{4}\phi_{12}''\left(a\right)-\beta\left(a\right)\right\}-\frac{R^2}{4}f\left(r\right)\right].$$

Hence

$$\varpi_2\left(r\right)=-H\left(a\right)+\bar{k}_2a^2\left\{1-\left(\frac{r}{a}\right)^2\right\}-R^2\left[\frac{1}{4}\phi_{12}''\left(a\right)-\beta\left(a\right)-\beta\left(r\right)-\frac{1}{4}a^2f\left(r\right)\left\{1-\left(\frac{r}{a}\right)^2\right\}\right].$$

We have restricted our analysis to the term of $O\left(R^2\right)$, therefore the time-averaged mean axial flow velocity is

$$\varpi\left(r\right)=-\varepsilon^2H\left(a\right)+\bar{k}a^2\left\{1-\left(\frac{r}{a}\right)^2\right\}-\varepsilon^2R^2\left[\frac{1}{4}\phi_{12}''\left(a\right)-\beta\left(a\right)-\beta\left(r\right)-\frac{1}{4}a^2f\left(r\right)\left\{1-\left(\frac{r}{a}\right)^2\right\}\right]. \tag{54}$$

The time averaged dimensionless flow rate $\overline{Q}/\pi ca_0^2$ is given by

$$\frac{\overline{Q}}{ca_0^2}=\varepsilon^2\frac{Q_{20}}{ca_0^2}=\varepsilon^2\int_0^a 2\pi\, r\varpi_2\left(r\right)\mathrm{d}r=\varepsilon^2\left[-\int_0^a 2\pi\, rH\left(a\right)\mathrm{d}r+\int_0^a 2\pi\, r\overline{k_2}\, a^2\left\{1-\left(\frac{r}{a}\right)^2\right\}\mathrm{d}r\right.$$
$$\left.-R^2\int_0^a 2\pi\, r\left\{\frac{1}{4}\phi_{12}''\left(a\right)-\beta\left(a\right)-\beta\left(r\right)-\frac{1}{4}a^2f\left(r\right)\left(1-\left(\frac{r}{a}\right)^2\right)\right\}\mathrm{d}r\right].$$

Or

$$\frac{Q_{20}}{\pi ca_0^2}=-a^2H\left(a\right)+\left\{-\frac{R}{4}\left(\frac{\mathrm{d}p}{\mathrm{d}z}\right)_2\right\}\frac{a^4}{2}-2R^2\int_0^a r\left\{\frac{1}{4}\phi_{12}''\left(a\right)-\beta\left(a\right)-\beta\left(r\right)-\frac{1}{4}a^2f\left(r\right)\left(1-\left(\frac{r}{a}\right)^2\right)\right\}\mathrm{d}r.$$

Therefore

$$\frac{a^4}{2}\bar{k}_2=\frac{Q_{20}}{\pi ca_0^2}+a^2H\left(a\right)+2R^2\int_0^a r\left\{\frac{1}{4}\phi_{12}''\left(a\right)-\beta\left(a\right)-\beta\left(r\right)-\frac{1}{4}a^2f\left(r\right)\left(1-\left(\frac{r}{a}\right)^2\right)\right\}\mathrm{d}r \tag{55}$$

so that

$$\frac{\mathrm{d}p}{\mathrm{d}z}=-\frac{8\varepsilon^2}{Ra^4}\left[\frac{Q_{20}}{\pi ca_0^2}+a^2H(a)+2R^2\int_0^a r\left\{\frac{1}{4}\phi_{12}''\left(a\right)-\beta\left(a\right)-\beta\left(r\right)-\frac{1}{4}a^2f\left(r\right)\left(1-\left(\frac{r}{a}\right)^2\right)\right\}\mathrm{d}r\right]. \tag{56}$$

Integrating Eq. (59) with respect to z from 0 to z, we get

$$\Delta p = -\frac{8}{R}\int_0^z \frac{1}{a^4}\left[\frac{\overline{Q}}{\pi c a_0^2} + \varepsilon^2 a^2 H(a) + 2\varepsilon^2 R^2 \int_0^a r\left\{\frac{1}{4}\phi_{12}''(a) - \beta(a) - \beta(r) - \frac{1}{4}a^2 f(r)\left(1-\left(\frac{r}{a}\right)^2\right)\right\}\mathrm{d}r\right]\mathrm{d}z. \tag{57}$$

Reflux occurs when $\omega_2(r) < 0$, which gives

$$k_2 < \frac{H(a) + R^2\left[\frac{1}{4}\phi_{12}''(a) - \beta(a) - \beta(r) - \frac{1}{4}a^2 f(r)\left\{1-\left(\frac{r}{a}\right)^2\right\}\right]}{a^2\left\{1-\left(\frac{r}{a}\right)^2\right\}}. \tag{58}$$

5. Long wave approximation

Now we study the situation in which $\alpha \ll 1$, i.e. the peristaltic wavelength is much greater than the pipe radius, keeping the Reynolds number arbitrary. If ε is also very small, the governing equations (24), (25) and (30) as well as the boundary and the regularity conditions (18)–(21) are valid here too. However unlike (32), the series representations of ϕ_1, ϕ_2, ϕ_3 and $\overline{k_2}$ involve α instead of R as listed below:

$$\begin{aligned}\phi_1 &= \phi_{10}^* + \alpha^2\phi_{12}^* + \cdots,\\ \phi_2 &= \alpha\phi_{21}^* + \alpha^3\phi_{22}^* + \cdots,\\ \phi_3 &= \phi_{30}^* + \alpha^2\phi_{32}^* + \cdots\end{aligned} \tag{32$'$}$$

where functions $\phi_{10}^*, \phi_{12}^*, \phi_{21}^*, \phi_{30}^*$ and ϕ_{32}^* are determined in exactly the same way as their corresponding functions without an asterisk.

The differential equations and boundary conditions of the quantities with an asterisk are the following:

$$L_0^2\left[\phi_{10}^*(r)\right] = 0, \tag{34$'$}$$

$$\phi_{10}^*(a) = \frac{1}{2}, \qquad \phi_{10}^{*'}(a) = \frac{k_0 a}{2} - \frac{1}{2a} \tag{35$'$}$$

$$L_0^2\left[\phi_{30}^*(r)\right] = 0 \tag{38$'$}$$

$$\begin{aligned}&L_0^2\left[\phi_{21}^*(r)\right] = -R\left[k_0\left(a^2-r^2\right)-1\right]L_0\left(\phi_{10}^*(r)\right)\\ &\phi_{21}^*(a) = \phi_{21}^{*'}(a) = 0,\end{aligned} \tag{47$'$}$$

$$\begin{aligned}&L_0^2\left[\phi_{12}^*(r)\right] = 2L_0\left[\phi_{10}^*(r)\right] + R\left[k_0\left(a^2-r^2\right)-1\right]L_0\left(\phi_{21}^*(r)\right) + R\,t_m\left\{k_0\left(a^2-r^2\right)-1\right\}L_0\left(\phi_{10}(r)\right)\\ &\phi_{12}^*(a) = \phi_{12}^{*'}(a) = 0.\end{aligned} \tag{48$'$}$$

The solution of (34′) is

$$\phi_{10}^*(r) = A_0^* r^3 + B_0^* r$$

where

$$A_0^* = -\frac{2-k_0a^2}{4a^3} \quad \text{and} \qquad B_0^* = \frac{4-k_0a^2}{4a}. \tag{59}$$

The solution of (47′) is

$$\phi_{21}^*(r) = A_1^* r^3 + B_1^* r + \frac{1}{24}A_0^* R\left[\left(1-k_0a^2\right)r^5 + \frac{k_0}{6}r\right] \tag{60}$$

where

$$A_1^* = \frac{1}{96a}\left(2-k_0a^2\right)R\left(2-\frac{3}{4}k_0a^2\right) \quad \& \qquad B_1^* = -\frac{1}{96}\left(2-k_0a^2\right)R\left(a-\frac{2}{3}k_0a^3\right).$$

Finally the solution of (48′) is

$$\phi_{12}^{*}(r) = A_2^{*}r^3 + B_2^{*}r + \frac{A_0^{*}}{12}r^5 - \frac{R}{24}\left[\left(1-k_0a^2\right)A_1^{*}r^5 + \left\{k_0A_1^{*} + \frac{R}{8}A_0^{*}\left(1-k_0a^2\right)^2\right\}\frac{r^7}{6} + \frac{R}{24}A_0^{*}\left\{\frac{k_0}{5}\left(1-k_0a^2\right)r^9 + \frac{k_0^2}{50}r^{11}\right\}\right] - \frac{1}{24}A_0^{*}R\,t_m\left[\left(1-k_0a^2\right)r^5 + \frac{k_0r^7}{6}\right], \tag{61}$$

where

$$A_2^{*} = -\frac{A_0^{*}}{6}a^2 + \frac{R}{24}\left[2\left(1-k_0a^2\right)A_1^{*}a^2 + \left\{\frac{k_0}{2}A_1^{*} + \frac{R}{16}A_0^{*}\left(1-k_0a^2\right)^2\right\}a^4\right] + \left(\frac{R}{24}\right)^2 A_0^{*}\left[\frac{4}{5}k_0\left(1-k_0a^2\right)a^6 + \frac{k_0^2}{10}a^8\right] + \frac{A_0^{*}R\,t_m}{24}\left[2\left(1-k_0a^2\right)a^2 + \frac{k_0a^4}{2}\right].$$

Differentiating (65) twice, with respect to r, we get

$$\phi_{12}^{*''}(a) = 6A_2^{*}a + \frac{5}{3}A_0^{*}a^3 - \frac{R}{24}a^3\left[20\left(1-k_0a^2\right)A_1^{*} + 7\left\{k_0A_1^{*} + \frac{R}{8}A_0^{*}\left(1-k_0a^2\right)^2\right\}a^2\right] - \left(\frac{R}{24}\right)^2 A_0^{*}\frac{k_0}{5}a^7\left\{72\left(1-k_0a^2\right) + 11k_0a^2\right\} - \frac{1}{24}A_0^{*}R\,t_m a^3\left[20\left(1-k_0a^2\right) + 7k_0a^2\right]. \tag{62}$$

Therefore

$$\varpi_2(r) = -H^{*}(a) + \bar{k}_2a^2\left\{1-\left(\frac{r}{a}\right)^2\right\} - \alpha^2\left[\frac{1}{4}\phi_{12}^{*''}(a) - \beta^{*}(a) - \beta^{*}(r) - \frac{1}{4}af^{*}(r)\left\{1-\left(\frac{r}{a}\right)^2\right\}\right] \tag{63}$$

and the mean axial velocity is

$$\varpi(r) = -\varepsilon^2H^{*}(a) + \bar{k}a^2\left\{1-\left(\frac{r}{a}\right)^2\right\} - \varepsilon^2\alpha^2\left[\frac{1}{4}\phi_{12}^{*''}(a) - \beta^{*}(a) - \beta^{*}(r) - \frac{1}{4}a^2f^{*}(r)\left\{1-\left(\frac{r}{a}\right)^2\right\}\right], \tag{64}$$

where

$$H^{*}(a) = \frac{1}{4}\left(\phi_{10}^{*''} - \frac{1}{a^2} - k_0\right) = \frac{k_0}{8} - \frac{1}{a^2}.$$

$$f^{*}(r) = \frac{r^2}{4}\left(\frac{R^2}{24}\right)\left[\frac{2-k_0a^2}{a^2}\left(\frac{8}{3}k_0a^2 - \frac{1}{12}k_0^2a^4 - 6\right) + \frac{3}{a^4}\left(1-k_0a^2\right)\left(8-6k_0a^2+k_0^2a^4\right)r^2 \times \frac{\left(2-k_0a^2\right)}{a^4}\left(10k_0 - 3k_0^2a^2 - \frac{4}{a^2}\right)r^4 - \frac{5k_0}{6a^6}\left(4-4k_0a^2+k_0^2a^4\right)r^6\right]$$

and

$$\beta^{*}(r) = \frac{r^2}{16}\left(\frac{R^2}{24}\right)\left[\frac{2-k_0a^2}{4a^2}\left(\frac{8}{3}k_0a^2 - \frac{1}{12}k_0^2a^4 - 6\right) + \frac{\left(1-k_0a^2\right)}{3a^4}\left(8-6k_0a^2+k_0a^4\right)r^2 + \frac{\left(2-k_0a^2\right)}{16a^4}\left(10k_0 - 3k_0^2a^2 - \frac{4}{a^2}\right)r^4 - \frac{k_0}{30a^6}\left(4-4k_0a^2+k_0^2a^4\right)r^6\right].$$

The pressure difference is given by

$$\Delta p = -\frac{8}{R}\int_0^z \frac{1}{a^4}\left[\frac{\overline{Q}}{\pi ca_0^2} + \varepsilon^2a^2H^{*}(a) + 2\varepsilon^2\alpha^2\int_0^a r\left\{\frac{1}{4}\phi_{12}^{*}{}''(a) - \beta^{*}(a) - \beta^{*}(r) - \frac{1}{4}a^2f^{*}(r)\left(1-\left(\frac{r}{a}\right)^2\right)\right\}\mathrm{d}r\right]\mathrm{d}z. \tag{65}$$

Reflux occurs when $\omega_2(r) < 0$, which gives

$$k_2 < \frac{H(a) + R^2\left[\frac{1}{4}\phi_{12}''(a) - \beta(a) - \beta(r) - \frac{1}{4}a^2f(r)\left\{1-\left(\frac{r}{a}\right)^2\right\}\right]}{a^2\left\{1-\left(\frac{r}{a}\right)^2\right\}}. \tag{66}$$

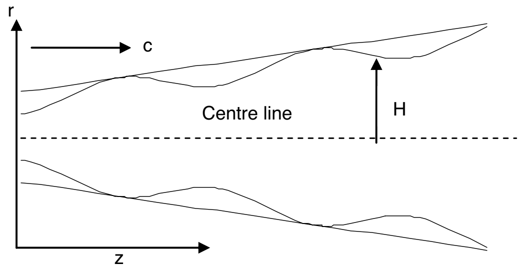

Fig. 1. Geometrical configuration of the circular cylindrical tube of varying cross section: z, r, c, h represent respectively axial coordinate, radial coordinate, wave velocity and wall distance from the centre line.

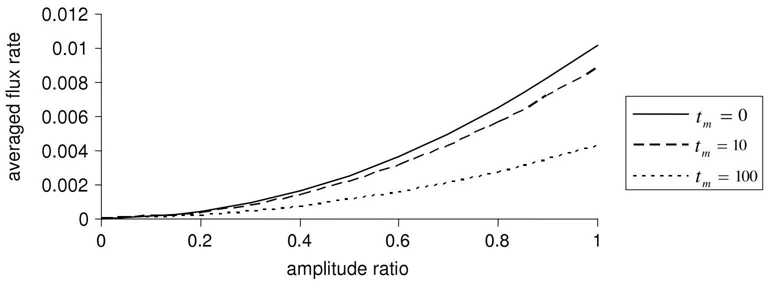

Fig. 2a. Diagram based on Eq. (57) shows the dependence of averaged flux rate on amplitude ratio for different values of relaxation time t_m ($\Delta p = 0$, $k = 0.0018$, $\alpha = 0.1$, $R = 0.1$).

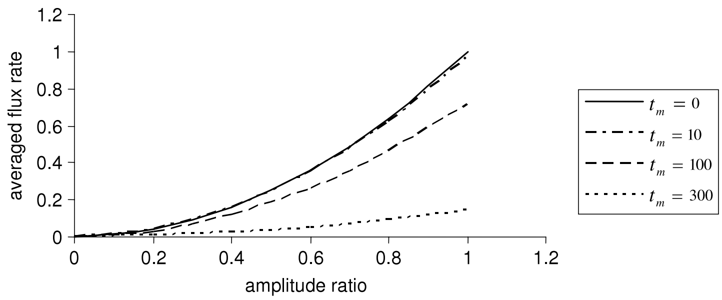

Fig. 2b. The diagram based on Eq. (65) shows the dependence of the averaged flux rate on the amplitude ratio for different values of the relaxation time t_m ($\Delta p = 0$, $k = 0.0018$, $\alpha = 0.1$, $R = 3$).

6. Numerical results and discussions

The analysis has been carried out to study the effects of relaxation time, the tapering of the tube and Reynolds number which is often neglected by considering creeping flows, on the flow pattern and when the fluid is of visco-elastic nature.

In order to apply the theoretical model to the flow through vas deferens we use its dimensions to evaluate the values of the parameters used in the analyses. The values based on the statistics presented by Guha et al. [15] for rhesus monkey are $L = 20$ cm, $a_0 = 0.0012$ cm, $\mu = 4$ cp. Based on these data the other parameters are evaluated as $\alpha = 0.00379$, $K = 0.0018$, $R = 3.0$. We further assume that the wavelength λ is equal to its length L and the wave velocity $c = 10$ cm/s (Fig. 1).

The case $k_0 = 0$ is called free pumping which means that the flow is purely peristaltic. Let the radius of the tube be given by $a(z) = a_0 + Kz$, where K is a parameter that represents the gradient of the tube. A plot between the amplitude ratio and the average flow rate given by Eq. (57) based on low Reynolds for different values of time relaxation t_m number reveals that the flow rate diminishes as the time relaxation parameter t_m increases at a given K (Fig. 2a). An almost identical revelation is observed when graphs are plotted from Eq. (65) which is based on long wave approximation (Fig. 2b). Revelations are similar when Δp is positive, which corresponds to an adverse pressure difference (Fig. 3), or negative, which gives favourable pressure difference (Fig. 4). The only difference observed is that the minimum flow rate is the one that is obtained by pressure difference imposed at the two ends of the tube. The positive and negative flow rates are obvious for favourable and adverse pressure differences respectively.

Figs. 5a and 5b illustrate the effect of time relaxation t_m on the axial velocity along the radial distance. It is observed that the axial velocity reduces as t_m increases. It may be, however, noted that t_m is effective only for large values. Fig. 5a is based on the assumption that the Reynolds number is low while the Fig. 5b is based on long wave approximation.

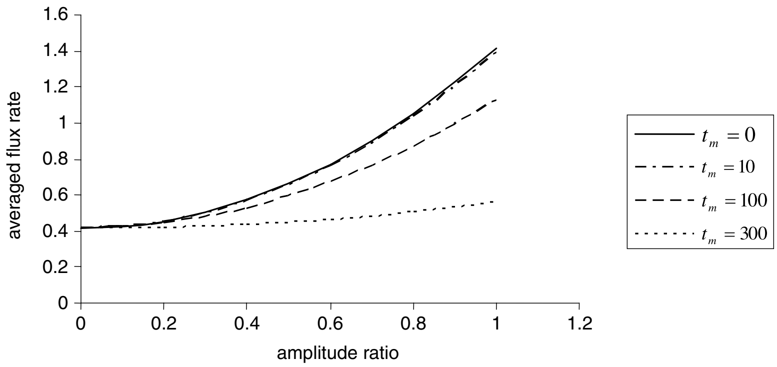

Fig. 3. Diagram based on Eq. (65) gives the dependence of averaged flux rate on amplitude ratio for different values of relaxation time $t_m(\Delta p = -200, K = 0.0018, \alpha = 0.1, R = 3)$.

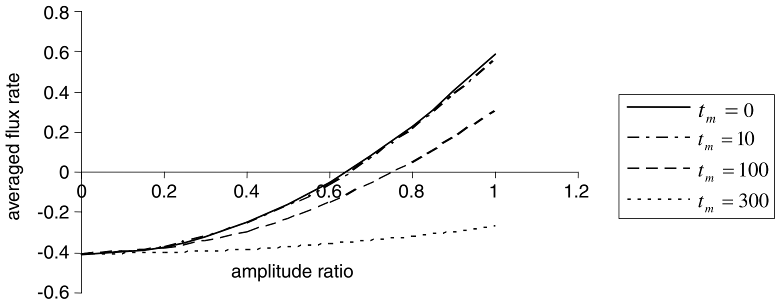

Fig. 4. Diagram based on Eq. (65) gives dependence of averaged flux rate on amplitude ratio for different values of relaxation time $t_m(\Delta p = 200, K = 0.0018, \alpha = 0.1, R = 3)$.

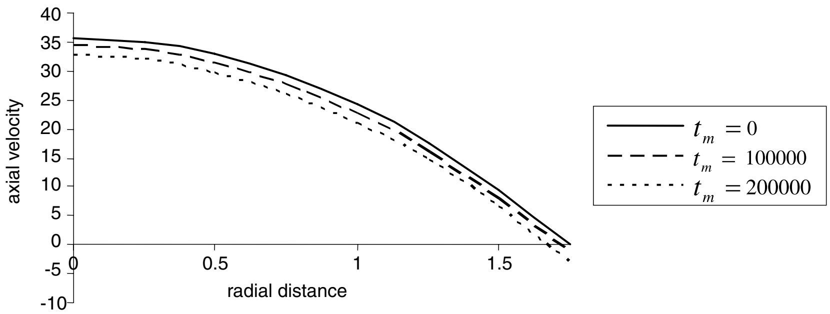

Fig. 5a. Diagram based on Eq. (54) shows dependence of axial velocity w on transverse distance r at a particular cross section for different values of relaxation time t_m ($\partial p/\partial z = -1869.40$, $z = 416.67$, $\alpha = 0.1$, $R = 0.1$, $K = 0.0018$).

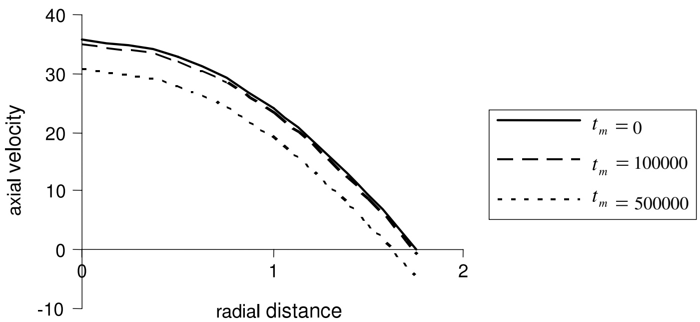

Fig. 5b. Diagram based on Eq. (64) shows the dependence of axial velocity w on transverse distance r at a particular cross section for different values of relaxation time t_m ($\partial p/\partial z = -1869.40$, $z = 416.67$, $\alpha = 0.1$, $R = 0.1$, $K = 0.0018$).

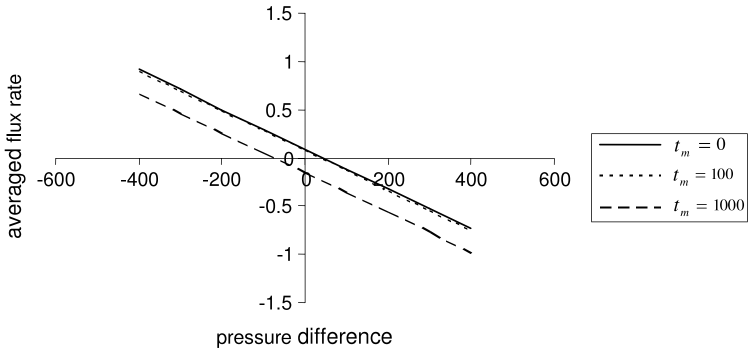

Fig. 6. Diagram based on Eq. (65) shows dependence of averaged flux rate on pressure difference of a non-uniform tube for different values of relaxation time t_m; other parameters are kept constant as $\varepsilon = 0.5$, $\alpha = 0.1$, $R = 3$, $K = 0.0018$.

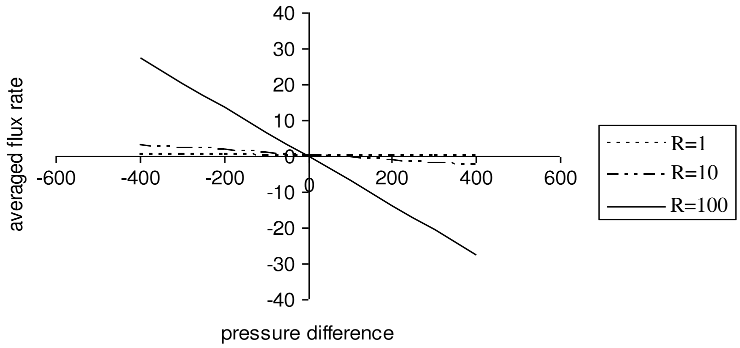

Fig. 7. Diagram based on Eq. (65) shows the dependence of averaged flux rate on pressure difference of a non-uniform tube for different values of the Reynolds number R. Other parameters are kept constant as $\varepsilon = 0.5$, $\alpha = 0.1$, $K = 0.0018$, $t_m = 0$.

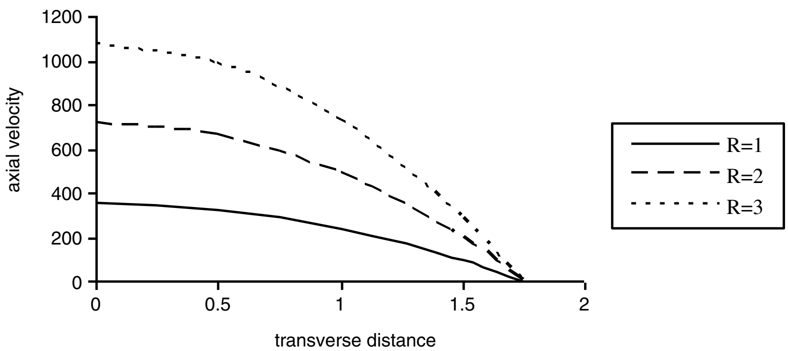

Fig. 8. Diagram based on Eq. (64) shows dependence of axial velocity w on transverse distance r at a particular cross section for different values of Reynolds number R ($\partial p/\partial z = -1869.40$, $z = 416.67$, $\alpha = 0.1$, $K = 0.0018$, $t_m = 0$).

The pressure difference and the average flow rate bear a linear relationship between them. When the time relaxation parameter increases, it is observed that the flow rate diminishes at the given pressure difference (Fig. 6), whereas the flow rate increases significantly when Reynolds number is increased. The difference is meagre when t_m is increased from 0 to 100; if it is further increased to 1000, the change is significant. One can infer from this that the flow rate of a visco-elastic fluid will be less than a Newtonian fluid under similar conditions (Fig. 7).

We study the effects of Reynolds number on the axial velocity by plotting graphs between the radial distance and the axial velocity (Fig. 8). It is observed that the axial velocity increases enormously with the Reynolds number when the pressure gradient, the wave number, the degree of tapering and the relaxation time are all kept constant.

It is further observed that the Reynolds number has very significant influence on the pressure distribution along the tube. The pressure difference decreases with increasing the Reynolds number when the wave number, the degree of tapering and the flow rate are kept fixed (Fig. 9). This clearly indicates the less the viscosity of the fluid pumped, the pump has to work less to propel the same quantity of the fluid.

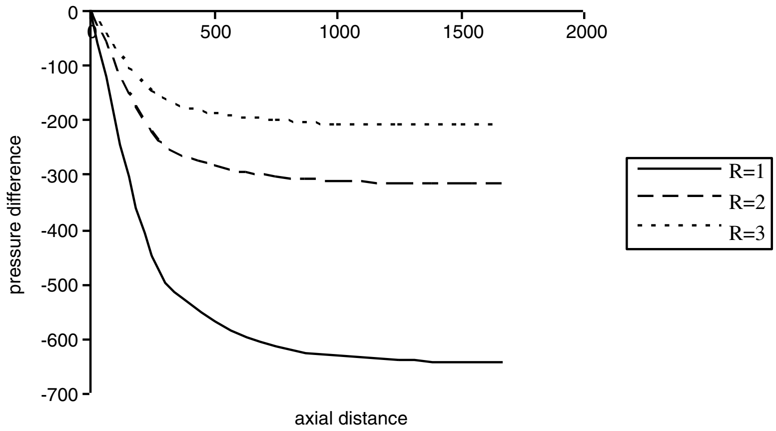

Fig. 9. Diagram based on Eq. (65) shows pressure distribution along axial distance for different values of Reynolds number R ($\alpha = 0.1, K = 0.0018, = 0, Q = 4.41$).

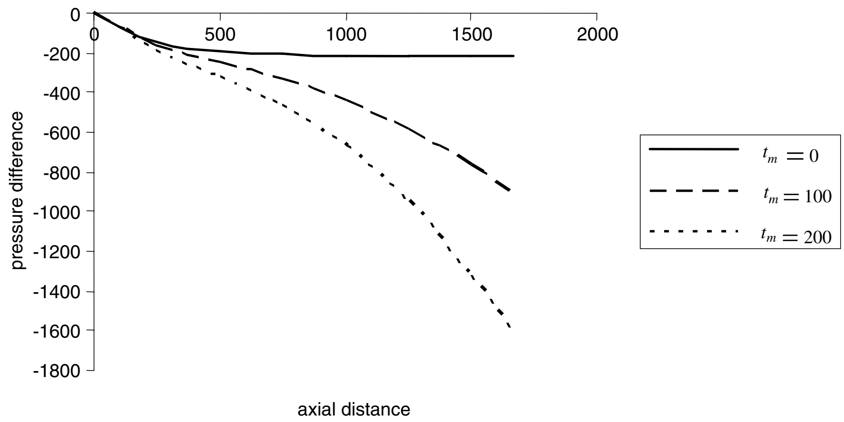

Fig. 10. Diagram based on Eq. (65) illustrates dependence of pressure on time relaxation t_m along the length of the tube for $\bar{Q} = 4.421, L = 1666.67$.

Fig. 10 illustrates the effect of time relaxation parameter t_m on the pressure for a fixed flow rate along the length of the tube. It is found that the pressure difference decreases as t_m increases. This is an indication that the pump has to work more to maintain the same flow rate when the fluid is visco-elastic.

In light of the aforementioned discussion it is inferred that the peristaltic contribution to the flow of seminal fluid, a visco-elastic fluid, in vas deference of rhesus monkey is slightly less than what was concluded by Misra and Pandey [5] under similar circumstances.

7. Conclusions

It is revealed that the flow rate diminishes as the time relaxation parameter increases at a given tapering parameter. Since the time relaxation parameter is the ratio of the viscosity to the elasticity, it may be interpreted as that the more elastic the fluid is, the less will be the flow rate. It is further disclosed that the axial velocity reduces when the fluid becomes more visco-elastic. However, this effect is reflected only for large values of the time relaxation parameter.

Another revelation is that the flow rate diminishes at the given pressure difference when the time relaxation parameter increases, whereas the flow rate increases significantly when Reynolds number is increased. The difference is meagre when t_m is increased from 0 to 100; if it is further increased to 1000, the change is significant. One can infer from this that the flow rate of a visco-elastic fluid will be less than a Newtonian fluid under similar conditions.

It is also concluded that the axial velocity increases enormously with Reynolds number while the pressure difference decreases with increasing Reynolds number for a fixed flow rate which may be interpreted as that the less the viscosity of the fluid pumped, the pump has to work less to propel the same quantity of a less viscous fluid. Moreover, the pressure decreases as t_m increases to maintain a fixed flow rate. It may be interpreted as that the pump has to work more to maintain the same flow rate of a visco-elastic fluid compared with a Newtonian fluid.

Acknowledgements

The authors acknowledge their indebtedness and gratefulness to the reviewers for their kind appraisal and suggestions to improve the presentation of the manuscript.

References

[1] T.W. Latham, Fluid motion in a peristaltic pump, M.S. Thesis, Massachusetts Institute of Technology, Cambridge, Massachusetts, 1966.
[2] B.B. Gupta, V. Seshadari, Peristaltic transport in non-uniform tubes, J. Biomech. 9 (1976) 105.
[3] L.M. Srivastava, V.P. Srivastava, Peristaltic transport of a non-Newtonian fluid: application to the vas deference and small intestine, Ann. Biomed. Eng. 13 (1985) 137.
[4] L.M. Srivastava, V.P. Srivastava, Peristaltic transport of a power-law fluid: application to the ductus efferentes of the reproductive tract, Rheol. Acta 27 (1988) 428.
[5] J.C. Misra, S.K. Pandey, Peristaltic transport in a tapered tube, Math. Comput. Modelling 22 (1995) 137.
[6] O. Eytan, A.J. Jaffa, D. Elad, Peristaltic flow in a tapered channel: application to embryo transport within the uterin cavity, Med. Eng. Phys. 23 (2001) 475.
[7] Kh.S. Mekheimer, Peristaltic transport of couple stress fluid in a uniform and non-uniform channels, Biorheology 39 (2002) 755.
[8] Kh.S. Mekheimer, Peristaltic flow of blood under effect of a magetic field in a non-uniform channel, Appl. Math. Comput. 153 (2004) 763.
[9] Kh.S. Mekheimer, Peristaltic transport of a Newtonian fluid through a uniform and non-uniform annulus, Arab. J. Sci. Eng. 30 (2005) 69.
[10] Kh.S. Mekheimer, Y.Abd. Elmaboud, Peristaltic transport of a particle-fluid suspension through a uniform and non-uniform annulus, Appl. Bionics Biomech. 5 (2008) 47.
[11] A.M. Sobh, Interaction of couple stresses and slip flow on peristaltic transport in uniform and non-uniform channels, Turkish J. Eng. Environ. Sci. 32 (2008) 117.
[12] P. Hariharan, V. Seshadri, R.K. Banerjee, Peristaltic transport of non-Newtonian fluid in a diverging tube with different wave form, Math. Comput. Modelling 48 (2008) 998.
[13] N. Ali, T. Hayat, S. Asghar, Peristaltic flow of a Maxwell fluid in a channel with compliant walls, Chaos Solitons Fractals 39 (2009) 407.
[14] O.H. Mahrenholtz, M.G. Mank, R.U. Zimmerman, The influence of wave form on peristaltic transport, Biorheology 15 (1978) 501.
[15] S.K. Guha, H. Kaur, A.M. Ahmed, Mechanism of spermatic flow in the vas deference, Med. Biol. Engg. 13 (1975) 518.